Double photoionization of argon into the $3s3p^5$ ^1P- and ^3P-states

B. Möbus[1], K.-H. Schartner[1], A. Ehresmann[2], H. Schmoranzer[2]

[1] I. Physikalisches Institut der Justus-Liebig-Universität, Heinrich-Buff-Ring 16, D-35392 Giessen, Germany
[2] Fachbereich Physik der Universität Kaiserslautern, Erwin-Schrödinger-Strasse, D-67663 Kaiserslautern, Germany

Abstract. Double photoionization of argon was studied by photon induced fluorescence spectroscopy (PIFS). Cross sections for the double photoionization into the $3s3p^5$ ^1P, ^3P states of Ar^{++} are presented for exciting photon energies between threshold and 120 eV. In the threshold range the energy dependencies of these cross sections were determined for the first time. Singlet and triplet states are populated with comparable probabilities at equal excess energies, in contrast to predictions of the extended Wannier theory. At $h\nu = 100$ eV the spin-orbit splitting of the $3s3p^5$ ^3P state was resolved, and a cross section for the production of Ar^{++} $3s^03p^6$ $^1S_0$ was determined for the first time.

PACS: 32.80.Fb

I. Introduction

Double photoionization at energies, where core hole formation and a following Auger effect are energetically prohibited, is a direct consequence of electron correlations [1, 2]. Therefore the double photoionization process gained and gains large interest. Early experimental studies in the seventies were not state selective and hence restricted to the determination of the total cross section or the ratio of the total cross section to the total single photoionization cross section [3–7].

From the theoretical point of view the approach concentrated on the He double photoionization [8], but calculations on the double photoionization of the other rare gases are scarce [1, 9]. Only the work of Carter and Kelly [9], based on many-body perturbation theory, distinguished the ns^2np^4- and the $nsnp^5$-configurations in the Ne and Ar double photoionization process. In the case of Ar they predicted a significant contribution of up to 25% of the $3s3p^5$-photoionization to the total double photoionization.

The first experimental investigations on the contribution of the s-electrons to the double photoionization

process in the rare gases were reported by Schartner et al. [10, 11]. Applying photon induced fluorescence spectroscopy (PIFS) to Ne and Ar they carried out state selective studies for the ^1P- and ^3P-components of the $nsnp^5$ configuration ($n = 2, 3$). Using photoelectron spectroscopy of single electrons Wehlitz [12] gave a partition of the double photoionization electron continuum of He, Ne, and Ar, based on calculated electron energy distributions [1, 9] and experimental ratios for the population of the different states [10, 13].

The question of a state selectivity of the double photoionization process was raised theoretically by [14] and experimentally by Lablanquie et al. [15]. The latter investigated the double photoionization into the ^3P-, ^1D-, and ^1S-states of the Ar^{++} $3s^23p^4$ ground state configuration and observed an exclusive population of the ^3P state. Their arguments supporting a state selectivity were based on the symmetry properties of the two-electron wavefunctions of the escaping electrons developed in the Wannier theory [14, 16–19]. In contrast, first in xenon [20] and later also in argon [13, 21–23] all final ionic states were experimentally found to be populated. The calculations of Huetz et al. [24] reduced the discussed final state selectivity to weak propensity rules. Recently, Hall et al. [25] used threshold photoelectron coincidence spectroscopy to obtain relative cross sections for the production of the different doubly charged states of ns^2np^4- and $nsnp^5$-configurations that are consistent with the results of Huetz et al. [24] except for the case of neon.

This paper describes the application of the PIFS to the Ar $3s3p^5$ ^1P- and ^3P-double photoionization. In comparison with the mentioned earlier investigation [10], in the new experiment described here a significant reduction of the uncertainties of the cross sections for the $3s3p^5$ ^1P- and ^3P-double photoionization was achieved. Above all we report the first state-selective study of the energy dependence of the argon $3s3p^5$ ^1P- and ^3P-double photoionization in the threshold region. We also present the first observation of the simultaneous photoionization of two $3s$-electrons leading to the Ar^{++} $3s^03p^6$ $^1S_0$ state.

II. Experimental method

PIFS is applicable to excited and radiating ions produced by the impinging photons. Studying the double photoionization process by PIFS has two main advantages. No coincidence measurements are necessary to distinguish between the various states of the doubly charged ion, and secondly the resolution in the fluorescence channel is independent of the bandwidth of the exciting photons. This is of importance especially near threshold. A survey of the method of PIFS is given by Schartner et al. [26].

Figure 1 shows schematically the experimental set-up used at the synchrotron radiation facility BESSY at Berlin. Some measurements were carried out at the toroidal-grating monochromator TGM 4 beam line, but for the measurements near the double photoionization thresholds the high flux at the wiggler/undulator TGM 5 beam line was necessary. The monochromatized synchroton radiation passed through a differentially pumped target cell, which contained the argon gas at a pressure of typically 10 mtorr. The impinging photon beam was monitored by the secondary-electron current of an aluminum cathode of 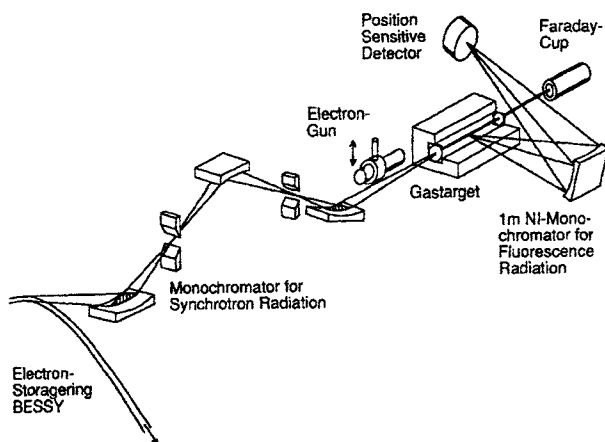a Faraday cup. The fluorescence radiation produced in the target region was observed perpendicular to the exciting photon beam. In our former applications of PIFS [10,27] we used a 0.5 m Pouey monochromator [28]. In order to obtain a higher resolution in the detection channel, this monochromator was replaced by a 1 m-normal incidence monochromator (McPherson 255). A special entrance slit head was used. It allows the exciting beam to lie as near as possible to the entrance slit of the monochromator. This was done to increase the solid angle of our experiment and thus the detection efficiency. Moreover the exit slit head was removed and a two-dimensional position sensitive detector was instead located in the focal plane of the monochromator. It consists of two channel-plates in front of a wedge-and-strip anode [29] and allows to simultaneously accumulate a spectral range of approximately 18 nm.

A detailed classification of the investigated transitions and their respective thresholds are given in Table 1. All observed transitions stem from photoionization processes, in which a $3s$-electron contributes. The simultaneous ionization of one s- and one p-electron leads to the Ar^{++} $3s3p^5$ ^1P- and $3s3p^5$ ^3P-states and the simultaneous ionization of two $3s$-electrons to the Ar^{++} $3s^02p^6$ ^1S state. The $3s$-single photoionization process leads to the 92.0, 93.2 nm doublet and was used for the normalization of the double photoionization cross sections.

Setting the entrance slit of the monochromator to 100 μm width a resolution of 0.1 nm in the fluorescence spectra was achieved. This is demonstrated in Fig. 2. At an excitation energy $hv = 100$ eV ($\Delta hv \approx 0.2$ eV) the spin orbit splitting of the $3s3p^5$ $^3P - 3s^23p^4$ ^3P multiplet around 88 nm was resolved. Fluorescence spectra with comparable resolution have been reported by Johnson et al. [32] and Samson et al. [33], but both studies used undispersed synchrotron radiation for excitation and a wavelength scan in the detection channel. To measure the low cross sections near the double photoionization thresholds the monochromator entrance slit was widely opened and the exciting photon beam served as the entrance slit of the normal incidence monochromator. In this mode the monochromator had a lower resolution depending on the foucussing of the exciting photons but its highest efficiency.

Fig. 1. Schematic view of the experimental set-up at the electron storage ring BESSY used for photon induced fluorescence spectroscopy

Table 1. Transitions observed by PIFS. Classifications according to Kelly [30] and Agentoft et al. [31] (for the $3s^03p^6$ $^1S_0$)

| Observed state	Binding energy	Observed transition	λ/nm
Ar II $3s3p^6$ $^2S_{1/2}$	29.24	$3s3p^6$ $^2S_{1/2} - 3s^23p^5$ $^1P_{1/2}$	93.205
		$3s3p^6$ $^2S_{1/2} - 3s^23p^5$ $^1P_{3/2}$	91.978
Ar III $3s3p^5$ $^3P_2$	57.50	$3s3p^5$ $^3P_2 - 3s^23p^4$ $^3P_1$	88.740
		$3s3p^5$ $^3P_2 - 3s^23p^4$ $^3P_2$	87.873
Ar III $3s3p^5$ $^3P_1$	57.62	$3s3p^5$ $^3P_1 - 3s^23p^4$ $^3P_0$	88.318
		$3s3p^5$ $^3P_1 - 3s^23p^4$ $^3P_1$	87.962
		$3s3p^5$ $^3P_1 - 3s^23p^4$ $^3P_2$	87.110
Ar III $3s3p^5$ $^3P_0$	57.69	$3s3p^5$ $^3P_0 - 3s^23p^4$ $^3P_1$	87.553
Ar III $3s3p^5$ $^1P_1$	61.25	$3s3p^5$ $^1P_1 - 3s^23p^4$ $^1D_2$	76.915
Ar III $3s^03p^6$ $^1S_0$	74.37	$3s^03p^6$ $^1S_0 - 3s3p^5$ $^1P_1$	94.52
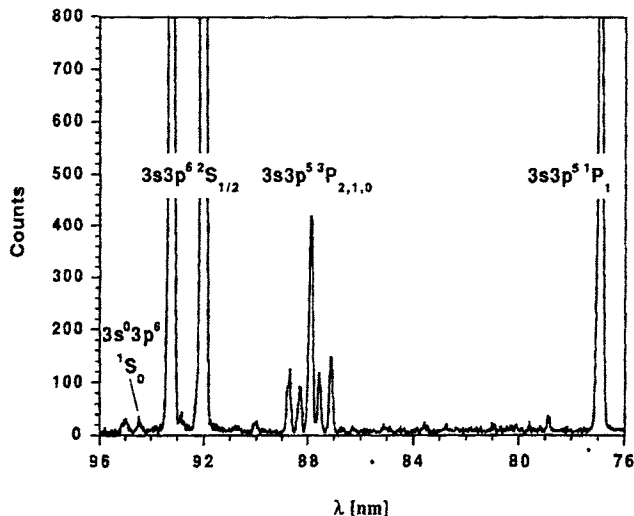
Fig. 2. Photon-induced fluorescence spectrum of Ar at $hv = 100$ eV excitation energy. The spectrum is not corrected for the detection efficiency. Only the upper levels of the observed transitions are given

Two modes of data accumulation were used. In the first mode, the multiplex mode, complete spectra at single excitation energies, sequentially increased, were recorded, i.e. all lines of interest were detected at the same time due to the ability of our position sensitive detector. The evaluation of cross sections from those spectra will be described in the following paragraph. In the second mode, the multiscaling mode, the signal of a single line was recorded and the exciting photon energy was repeatedly scanned. Additionally to each scan, a single spectrum in the multiplex mode was accumulated and used to put the measured relative cross sections on an absolute scale (see below). Of course this mode was more time consuming but expected to be less sensitive to possible drifts of experimental parameters.

A spectrum like in Fig. 2 yields the fluorescence intensity of the state of interest in relation to the intensity at $\lambda = 92.0$ nm, a fluorescence following the $3s$-single photoionization. Knowing the cross section $\sigma\,(3s\,3p^6\,{}^2S)$ of the latter process [34] and the detection efficiencies at the different wavelengths with respect to the detection efficiency at $\lambda = 92$ nm, one obtains the cross section of interest. To get these relative detection efficiencies, we replaced the exciting photon beam in-situ by an electron beam (Fig. 1) and accumulated an electron impact induced fluorescence spectrum. From the measured intensity ratios within this spectrum and the known ratios of the respective cross sections for the electron impact induced fluorescence we obtained the relative detection efficiencies. This method, named *radiometric standard based on electron impact induced line radiation* (RASTELLI), was described in detail by Schartner et al. [35]. Cross sections for the radiation at 92.0, 93.2, and 76.9 nm were measured by Jans [36] with low uncertainties of $\pm 6\%$. Resolution of the $3s\,3p^5\,{}^3P - 3s^2\,3p^4\,{}^3P$ multiplet, as shown in Fig. 2, was necessary to apply this method in the region around 88 nm. In this case one has

to single out the transition at 88.3 nm, the only transition in the electron impact induced spectrum free from any blends. The cross section of this emission line was given by Kraus [37]. The described procedures lead to total uncertainties of $\pm 20\%$, $\pm 27\%$, and $\pm 24\%$ for $\sigma\,(3s\,3p^5\,{}^1P)$, $\sigma\,(3s\,3p^5\,{}^3P)$, and $\sigma\,(3s\,3p^5\,{}^1P+{}^3P)$, respectively, essentially reduced when compared with [10]. An extrapolation of the relative detection efficiencies at 88.3, 92.0 and 93.2 nm yields the value at 94.5 nm, leading to a total uncertainty of $\pm 50\%$ for $\sigma\,(3s^0\,3p^6\,{}^1S)$.

Our stated uncertainties do not take into account the possible anisotropic angular distribution of the observed intensities. At higher energies a correction will be negligible within the uncertainties mentioned above. This follows from the relative intensity distribution within the $3s^2\,3p^4\,{}^3P - 3s\,3p^5\,{}^3P$ multiplet around 88 nm (Fig. 2), which is in agreement with the relative intensity distribution resulting from the assumption of a statistical population of the states within the LS-coupling scheme. We assume the same to hold for the transition from the ${}^1P$ state. Near threshold, further investigations of a possible alignment should be carried out which were hampered at the present status of our experiment by the low count rates.

III. Results and discussion

Cross sections $\sigma\,(3s\,3p^5\,{}^1P)$, $\sigma\,(3s\,3p^5\,{}^3P)$ and the sum $\sigma\,(3s\,3p^5\,{}^1P+{}^3P)$ for the argon double photoionization in the region near threshold are presented in Fig. 3. Figure 4 shows these cross sections from threshold up to 120 eV. The dots and small crosses in Fig. 3 are mean values from a number of measurements in the multiplex mode for the single ${}^3P$- and ${}^1P$-lines, respectively. The
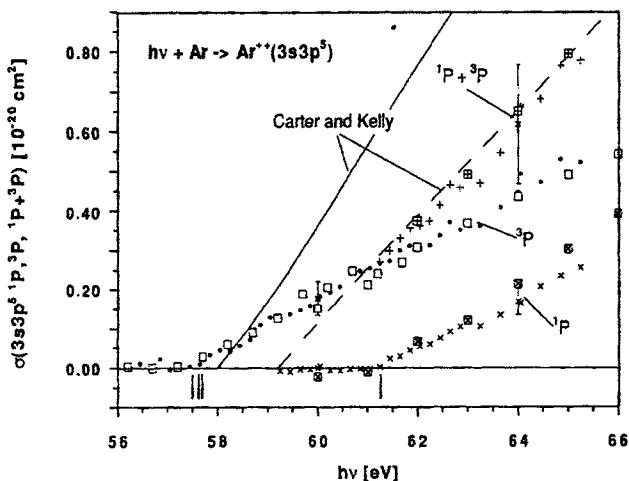

Fig. 3. Photoionization cross sections in the threshold region as function of the exciting photon energy. This work: $\times$, ⊠ $\sigma\,(3s\,3p^5\,{}^1P)$; ●, ⊡ $\sigma\,(3s\,3p^5\,{}^3P)$; $+$, ⊞ $\sigma\,(3s\,3p^5\,{}^1P+{}^3P)$ (identical to $\sigma\,(3s\,3p^5\,{}^3P)$ below 61.25 eV); $+$, ●, $\times$ stem from measurements in the multiplex mode; ⊠, ⊡, ⊞ stem from measurements in the multiscaling mode; Carter and Kelly [9]: —— length and ——— velocity form results for $\sigma\,(3s\,3p^5\,{}^1P+{}^3P)$
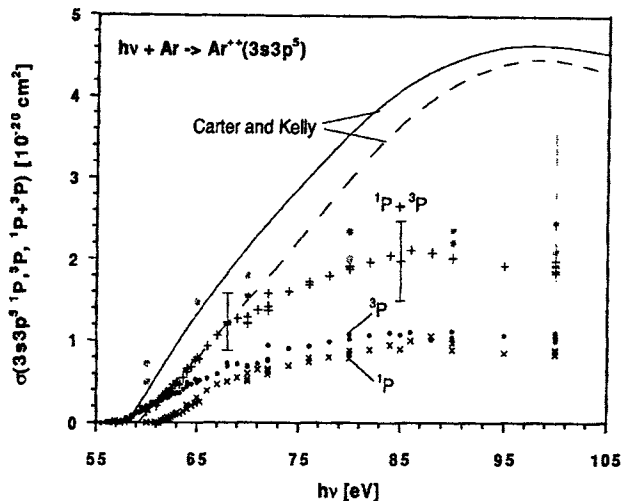
Fig. 4. Photoionization cross sections as function of the exciting photon energy: This work: × $\sigma(3s3p^5\,^1P)$; ● $\sigma(3s3p^5\,^3P)$; + $\sigma(3s3p^5\,^1P+^3P)$; Schartner et al. [10]: ● (shown greyed) $\sigma(3s3p^5\,^1P+^3P)$; Cartner and Kelly [9]: —— length and ——— velocity form results for $\sigma(3s3p^5\,^1P+^3P)$

plus symbols mark the sum of these data. The remaining symbols in Fig. 3 result from measurements in the multiscaling mode. For the ^3P state a very good agreement between the multiplex mode and the multiscaling mode data is present while for the ^1P state differences are visible in Fig. 3, which are not understood so far. Our early data [10] have been inserted in Fig. 4 for comparison. The agreement between both data sets is rather satisfactory except for the low energies.

Our determination of cross sections in the threshold region of the $3s3p^5\,^1P$- and ^3P-double photoionization as shown in Fig. 3 was stimulated by the controversial discussion of a possible final-state selectivity in the case of the Ar $3s^23p^4\,^3P$-, ^1D-, and ^1S-double photoionization as outlined in the introduction. In the following we discuss the formation of the $3s3p^5\,^1P$- and ^3P-states within the context of the Wannier model as it was used in [13, 15, 20-22, 25]. Therein what is called the Wannier model is a combination of classically determined electron emission characteristics dominated by the Wannier ridge and of symmetry properties of the quantum mechanical wave function of the two escaping electrons. In the case of Ar we start from the $3s^23p^6$ ground state of $^1S^e$ symmetry. For an electric dipole transition the final state is of $^1P^0$ symmetry. Thus the $3s3p^5\,^1P^0$ ionic state combines with $^1S^e$-, $^1P^e$-, and $^1D^e$-states of the two-electron wave function, while the $^3P^0$ ionic state combines with the $^3P^e$-, $^3S^e$-, and $^3D^e$-states of the two-electron wave function. A selective mechanism on the basis of kinematically disfavoured partial waves and higher Wannier exponents [14, 17-19] would prefer the $^1S^e$- and $^1D^e$-two-electron states and thus favour the formation of the $^1P^0$ ionic state of the $3s3p^5$ configuration.

As shown in Fig. 3 the measured cross sections for the ^1P- and ^3P-states are of comparable magnitude at equal excess energies. There is no experimental evidence for a preferential population of the ^1P state in contrast to the

argumentation outlined above. Our result is also in contrast to the recent experimental result of Hall et al. [25]. Using threshold photoelectron coincidence spectroscopy they found a preferential but not exclusive population of the ^1P state at threshold for Ar. But for Ne and Kr their spectra show comparable population of the ^1P- and ^3P-states.

Indications for an indirect population of doubly ionized states via the autoionization of $nsnp^5(^1P)nl$ satellite states were found in the studies of [13, 20-23, 25, 38]. At present a quantitative discussion of this cascade effect is not possible since cross sections for the production of the $nsnp^5(^1P)nl$ satellites are unknown. From calculated autoionization rates [39] it follows that the indirect population of the $nsnp^5\,^3P$ state should be stronger for Ne than for Ar since in the case of Ar the autoionization to $3s^23p^4$ Ar^{++} ground states is preferred. Nevertheless at the thresholds of the $nsnp^5(^1P)nl$ satellite states an indirect population of doubly ionized states should lead to structures superimposed on the energy dependence of the cross sections of the latter. This was found in Ne [11] but, as shown in Fig. 3, the cross sections measured in the present study rise practically linearly from the thresholds on, indicating the weakness of the indirect population.

Comparing the data and the theoretical predictions we have to consider the following: In our opinion the extended Wannier theory is not applicable as outlined above. First a complete description of the angular distribution pattern is necessary but not available for the $3s3p^5$ double photoionization. For the $3s^23p^4$ double photoionization Huetz et al. [24] calculated form factors for the so-called favoured and unfavoured states leading to weak propensity rules rather than to strong selection rules. Secondly the mentioned symmetry considerations should be applied only within the same ionic state, otherwise core effects have to be considered. Speaking within the Wannier theory detailed calculations in the reaction zone are needed. A further explanation might be that our data – though being close to threshold – are still above the range of validity of a threshold law for a state selectivity. This would explain also the difference with the observation at threshold made by Hall et al. [25].

To our knowledge the only calculations of cross sections for the $3s3p^5$ double photoionization process were performed by Carter and Kelly [9] within the many-body pertubation theory. Their results are inserted in Fig. 3 for the threshold range and in Fig. 4 for energies from threshold up to 100 eV. Carter and Kelly's data, which hold for the sum $\sigma(3s3p^5\,^1P+^3P)$, were reproduced from Fig. 3 of [9]. Since the calculation does not treat the ^3P- and ^1P-channels separately, it cannot reproduce the details of Fig. 3, i.e. the change of the slope of $\sigma(3s3p^5\,^1P+^3P)$ at the onset of the ^1P channel. The agreement between our summed experimental cross sections and the calculated velocity form results above this onset is certainly fortuitous since velocity and length form results considerably differ at the energies displayed in Fig. 3. At the higher energies of Fig. 4 where both formulations agree reasonably well with each other, the cal-

culated result is by a factor of two higher than our experimental data. Moreover the calculation predicts a cross section maximum around $h\nu = 95$ eV while our experimental data have the largest values around $h\nu = 85$ eV.

Our present data for the $3s\,3p^5$ photoionization cross section show that the contribution of the $3s$-electrons to the double photoionization needs further theoretical consideration. This holds for the calculation of the angular distribution pattern to yield a complete description of the $3s\,3p^5$ photoionization process within the Wannier theory as well as for the calculation of the matrix elements for the $3s\,3p^5$ double photoionization process. Similar to the relation between the $3s$- and $3p$-single photoionization, the double photoionization into the $3s\,3p^5$ continuum is a weaker channel with respect to the photoionization into the $3s^2\,3p^4$ continuum and is in a comparable way more sensitive to higher-order effects of the electron correlations. E.g. the satellite channels $3s^2\,3p^3\,nl$ which open energetically above $h\nu = 65$ eV could influence the $3s\,3p^5$ photoionization process. To our knowledge they are not included in the mentioned MBPT calculations but calculations of the binding energies of Ar III states within the configuration-interaction theory by Hansen and Persson [40] demonstrated a strong mixing of $3s\,3p^5\,{}^1P$- and ${}^3P$-states with $3s^2\,3p^3({}^2D)3d\,{}^1P$- and ${}^3P$-states and weaker mixing with $3s^2\,3p^3({}^2P)4s\,{}^1P$- and ${}^3P$-states. A first experimental evidence for the population of one of the mentioned states, namely the $3s^2\,3p^3({}^2P)4s\,{}^3P$ state, can be found in a fluorescence spectrum published by Samson et al. (Fig. 3b in [33]). Further experimental and calculational efforts are clearly necessary to illuminate this aspect of double photoionization.

The double photoionization cross section for the two $3s$-electrons is probably even more sensitive to higher-order effects. This process was observed for the first time in the present study but only at a single photon energy of $h\nu = 100$ eV. A cross section of 0.6 kb with an uncertainty of 50% was measured for this energy. The only theoretical value can be derived on the basis of the shake theory in the sudden approximation. Carlson and Nestor [41] gave a probability of 0.16% for the shake-off of a $3s$-electron provided a $3s$-electron vacancy was produced in advance. From the $3s$-photoionization cross section at $h\nu = 100$ eV a value of 0.22 kb follows for the shake-off double photoionization of the two $3s$-electrons. This result is in disagreement with the measured value. On the other hand it is certainly doubtful if the sudden approximation can be tested at an energy of 25 eV above the threshold and for electrons of the same shell as already mentioned by [41].

IV. Summary

Summarizing, cross sections for the double photoionization of Ar into the $3s\,3p^5\,{}^1P$- and ${}^3P$-states were measured for exciting photon energies from threshold up to $h\nu = 100$ eV and for the $3s^0\,3p^6\,{}^1S$ state at $h\nu = 100$ eV in order to provide a quantitative basis for studies of the electron correlations that are responsible for the double photoionization process. Near threshold no preferential

population of the ${}^1P$ state was observed as predicted by the extended Wannier theory and observed by the threshold photoelectron coincidence spectroscopy. At higher energies the only existing predictions, calculated within the MBPT, overestimate the sum of the cross sections for the ${}^1P$- and ${}^3P$-states by a factor of approximately two. Further experimental and calculational efforts are clearly necessary for a correct description of the double photoionization process.

References

1. Chang, T.N., Poe, R.T.: Phys. Rev. A16, 1432 (1975)
2. Amusia, M.Ya.: Comm. At. Mol. Phys. 10, 155 (1981)
3. West, J.B., Marr, G.V.: Proc. R. Soc. London A349, 397 (1976); Marr, G.V., West, J.B.: At. Data Nucl. Data Tables 18, 497 (1976)
4. Carlson, T.A.: Phys. Rev. 156, 142 (1967)
5. Samson, J.A.R., Haddad, G.N.: Phys. Rev. Lett. 33, 875 (1974)
6. Schmidt, V., Sandner, N., Kuntzemüller, H., Dhez, P., Wuilleumier, F., Källne, E.: Phys. Rev. A13, 1748 (1976)
7. Holland, D.M., Codling, K., West, J.B., Marr, G.V.: J. Phys. B12, 2465 (1979)
8. Schmidt, V.: Rep. Prog. Phys. 55, 1483 (1992)
9. Carter, S.T., Kelly, H.P.: Phys. Rev. A16, 1525 (1977)
10. Schartner, K.-H., Lenz, P., Möbus, B., Schmoranzer, H., Wildberger, M.: Phys. Lett. A128, 374 (1988)
11. Schartner, K.-H., Mentzel, G., Magel, B., Möbus, B., Ehresmann, A., Vollweiler, F., Schmoranzer, H.: J. Phys. B26, L445 (1993)
12. Wehlitz, R.: Ph. D. Thesis, Technische Universität Berlin 1991
13. Price, S.D., Eland, J.H.D.: J. Electron Spectrosc. Relat. Phenom. 52, 649 (1990)
14. Klar, H., Schlecht, W.: J. Phys. B9, 1699 (1976)
15. Lablanquie, P., Eland, J.H.D., Nenner, I., Morin, P., Delwiche, J., Hubin-Franskin, M.-J.: Phys. Rev. Lett. 58, 992 (1987)
16. Wannier, G.: Phys. Rev. 90, 817 (1953)
17. Greene, C.H., Rau, A.R.P.: Phys. Rev. Lett. 48, 533 (1982)
18. Greene, C.H., Rau, A.R.P.: J. Phys. B16, 99 (1983)
19. Stauffer, A.D.: Phys. Lett. 91A, 114 (1982)
20. Price, S.D., Eland, J.H.D.: J. Phys. B22, L153 (1989)
21. Hall, R.I., McConkey, A., Ellis, K., Dawber, G., MacDonald, M.A., King, G.C.: J. Phys. B25, 799 (1992)
22. Krässig, B., Schmidt, V.: J. Phys. B25, L327 (1992)
23. Krässig, B., Schwarzkopf, O., Schmidt, V.: J. Phys. B26, 2589 (1993)
24. Huetz, A., Selles, P., Waymel, D., Mazeau, J.: J. Phys. 24, 1917 (1991)
25. Hall, R.I., Dawber, G., McConkey, A.G., MacDonald, M.A., King, G.C.: Z. Phys. D23, 377 (1992)
26. Schartner, K.-H., Lenz, P., Möbus, B., Magel, B., Schmoranzer, H., Wildberger, M.: Phys. Scr. 41, 853 (1990)
27. Schartner, K.-H., Lenz, P., Möbus, B., Schmoranzer, H., Wildberger, M.: J. Phys. B22, 1573 (1989)
28. Schmoranzer, H., Molter, K., Noll, T., Imschweiler, J.: Nucl. Instrum. Methods A246, 485 (1986)
29. Kraus, B., Schartner, K.-H., Folkmann, F., Livingston, A.E., Mokler, P.H.: In: Hailey, C.J., Siegmund, H.W. (eds.). Proc. SPIE, Vol. 1159. Bellingham, Soc. Photo. Opt. Instrum. Eng. p. 217 (1989); Kraus, B.: Ph.D. Thesis, Universität Gießen (1991), published as: GSI Report 91-16. Darmstadt, Gesellschaft für Schwerionenforschung mbH (1991)

30. Kelly, R.L.: J. Phys. Chem. Ref. Data **16**, [Suppl. 1] (1987)
31. Agentoft, M., Andersen, T., Hansen, J.E., Persson, W., Petterson, S.-G.: Phys. Scr. **29**, 57 (1984)
32. Johnson, B.M., Meron, M., Agagu, A., Jones, K.W.: Nucl. Instrum. Methods **B24/25**, 391 (1987)
33. Samson, J.A.R., Chung, Y., Lee, E.-M.: Phys. Lett. **A127**, 171 (1988)
34. Möbus, B., Magel, B., Schartner, K.-H., Langer, B., Becker, U., Wildberger, M., Schmoranzer, H.: Phys. Rev. **A47**, 3888 (1993)
35. Schartner, K.-H., Kraus, B., Pöffel, W., Reymann, K.: Nucl. Instrum. Methods **B27**, 519 (1987)
36. Jans, W.: Ph. D. Thesis, Technische Universität Berlin 1993
37. Kraus, B.: Diploma Thesis, Universität Gießen 1986 (unpublished)
38. Pahler, M., Caldwell, C.D., Schaphorst, S.J., Krause, M.O.: J. Phys. **B26**, 1617 (1993)
39. Armen, G.B., Larkins, F.P.: J. Phys. **B24**, 741 (1991)
40. Hansen, J.E., Persson, W.: J. Phys. **B20**, 693 (1987)
41. Carlson, T.A., Nestor, C.W.: Phys. Rev. **A8**, 2887 (1973)